

## Terahertz quantum cascade lasers with silver- and gold-based waveguides

R. A. Khabibullin<sup>1</sup>, N. V. Shchavruk<sup>1</sup>, D.S. Ponomarev<sup>1</sup>, D.V. Ushakov<sup>2</sup>,  
 A.A. Afonenko<sup>2</sup>, O.Yu. Volkov<sup>3</sup>, V.V. Pavlovskiy<sup>3</sup>, A.A. Dubinov<sup>4</sup>

<sup>1</sup>V.G. Mokerov Institute of Ultra High Frequency Semiconductor Electronics of RAS, Moscow, Russia,

[khabibullin@isvch.ru](mailto:khabibullin@isvch.ru)

<sup>2</sup>Belarusian State University, Minsk, Belarus

<sup>3</sup>Institute of radio-engineering and electronics of RAS, Moscow, Russia

<sup>4</sup>Institute for Physics of Microstructures RAS, Nizhny Novgorod, Russia

For the practical use of THz quantum cascade lasers (QCLs) in a large field of applications, including real-time THz imaging and THz spectroscopy, it is necessary to develop low loss waveguides [1]. The most efficient in the THz region of the spectrum is a double metal waveguide (DMW) design in which the active region is placed between two metal layers. The mode confinement factor in such waveguides is  $\Gamma \sim 1$ , which is much higher than in plasmon waveguides ( $\Gamma \sim 0.3$ ), which effectively work for mid-infrared QCLs. However, QCLs with DMW are complex in fabrication [2] and require preliminary theoretical and experimental studies of the behavior of the dielectric constant and the loss coefficient of both metals and semiconductors in the THz spectral region.

For the development of more efficient laser schemes for THz QCLs, as well as a low loss waveguide design, the information is needed on the loss in THz QCLs over a wide range of temperatures and frequencies. It is shown that the loss in THz QCLs plays an important role in the internal tuning of the radiation frequency [3]. In this work, we propose to use a double metal waveguide based on silver (Ag), for reducing the losses of the waveguide. In comparison with Au, Ag has a higher electrical and thermal conductivities, which should lead to low losses in the Ag-based waveguide. For this purpose, we investigate the spectra of mode losses in THz QCL with DMW based on Au and Ag.

Metal film of Ti/Au (30/1000 nm) and Ti/Ag (30/1000 nm) are deposited on SI-GaAs, and their resistivities are measured using Van der Pauw method in the temperature range from 4.2 to 300 K. The dielectric constants and loss coefficients ( $\alpha_{\text{met}}$ ) are calculated on the basis of measurements of the resistivity of metals using the Drude model. As shown in Fig. 1, the loss coefficient on the Au- and Ag-based DMW increases with increasing frequency and temperature. Using Ag for DMW allows to reduce  $\alpha_{\text{met}}$  by more than  $2 \text{ cm}^{-1}$  comparing with DMW based on Au.

Calculations of the coefficient of total losses, including losses on the DMW, resonator mirrors, optical phonons and free charge carriers, are performed for a  $10\text{-}\mu\text{m}$  waveguide. It is demonstrated that, taking into account the absorption of THz radiation by free carriers and optical phonons (see the inset of Fig. 2), the spectrum of total mode losses has a wide minimum in the region of 3-6 THz, which shifts to the high-frequency region of the spectrum with increasing temperature (see Fig. 2). The minimum losses in an Au-based waveguide with an increase of temperature

from 100 to 300 K increase from 8 to  $27 \text{ cm}^{-1}$ . The use of Ag-based DMW allows to reduce losses by 2–4  $\text{cm}^{-1}$  in comparison with Au-based DMW.

We have designed the active region of the THz QCL based on three tunnel-coupled quantum wells GaAs/Al<sub>0.15</sub>Ga<sub>0.85</sub>As with a resonance-phonon depopulation scheme [4]. Numerical calculations of energy levels, matrix elements of dipole transitions, the degree of subbands populations and gain spectra are carried out depending on the applied electric field and temperature. It is shown that the maximum gain is realized under phonon resonance conditions at a frequency of 3.37 THz at an electric field strength of  $F = 12.3 \text{ kV/cm}$  [5].

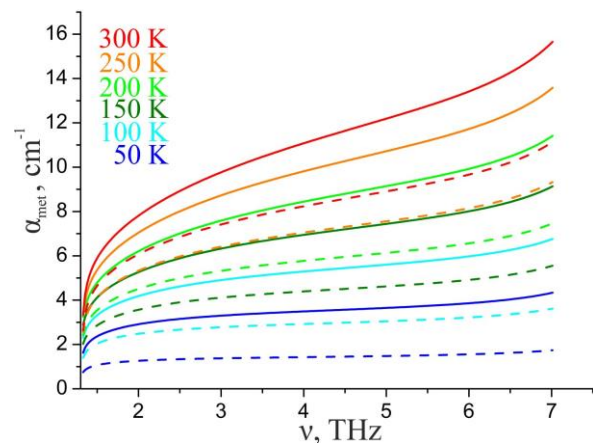


**Fig. 1.** The spectra of the loss coefficient on the Au-based DMW (solid lines) and Ag-based DMW (dashed lines) at temperatures from 50 to 300 K.

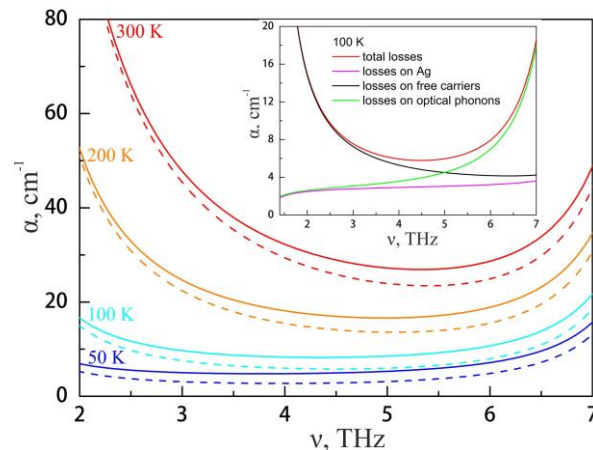


**Fig. 2.** Total losses of THz QCL with DMW based on Au and Ag for different temperatures. The inset shows the components for the total loss coefficient for THz QCL based on Ag DMW at 100 K.

Based on the proposed design, the laser heterostructures are grown by molecular beam epitaxy with 10  $\mu\text{m}$  active region thickness [6]. We fabricate ridge structures with Au-based DMW [7]. The device is die bonded to a copper submount with wire bonding to ridge structures. Measurements are made with an abutted to laser facet sapphire hyperhemispherical lens.

The lasing threshold of the fabricated THz QCL is achieved at a current of 0.85–0.86 A for 20 K. The influence of temperature on the threshold current and output power of the fabricated THz QCL emitting near  $\sim 3.3$  THz with a maximum operating temperature of  $T_{\text{max}} \sim 84$  K is investigated. By fitting the dependence of threshold current  $J_{\text{th}}$  on temperature to the empirical expression  $J_{\text{th}} \sim \exp(T/T_0)$ , we obtain the characteristic temperature  $T_0 = 20$  K for fabricated THz QCL. It is seen that with an increase in temperature from 40 to 58 K, an insignificant decrease in the THz QCL radiation power by  $\sim 35\%$ , which allows the pumping of nitrogen vapors to be used to cool the laser. The characteristic energy of  $E_a = 23$  meV, which is necessary for the temperature activation of LO phonon emission in the case of electron recombination from the upper laser level to the lower one, is determined from the Arrhenius temperature dependence of the output power.

In measured at 58 K spectrums, there are three equidistant spectral lines corresponding to the longitudinal Fabry-Perot modes with  $\Delta f = c/2nL = 40$  GHz for  $L=1$  mm. The mode content varies with the bias current. There are three radiation modes (3.24, 3.28, 3.32 THz) at a pumping current of 0.940 A. Generation at 3.32 THz ceases when the current increases to 1.005 A, and only two high-frequency modes remain at 1.058 A. The maximum amplitude of the total radiation power is 28  $\mu\text{W}$  in the 3.25–3.32 THz range at a temperature of 42 K [8].

We investigate the post-growth processing for THz QCL with Ag-based DMW. This processing includes the Ag–Ag thermocompression bonding of QCL heterostructures with a doped n+-GaAs substrate, mechanical lapping and selective wet etching of the substrate, and dry etching of QCL ridge structures through a Ti/Ag/Au metallization mask 100  $\mu\text{m}$  wide. Reactive-ion-etching recipe with an inductively coupled plasma source in a  $\text{BCl}_3/\text{Ar}$  gas mixture is selected to obtain vertical walls of the QCL ridge structure with minimum Ti/Ag/Au mask sputtering (Fig. 6).

### Conclusion

The coefficient of total losses of THz QCL with DMW based on Au and Ag have been analyzed. We have designed and fabricated THz QCLs with Au-DMW based on  $\text{GaAs}/\text{Al}_{0.15}\text{Ga}_{0.85}\text{As}$  three-quantum well active module with resonant-phonon depopulation scheme. We investigate the dependence of threshold current and lasing output power on temperature. The dependence of the radiation spectrum on the amplitude of the excitation current pulse was investigated. The postgrowth processing for THz QCL with Ag-based DMW are studied.

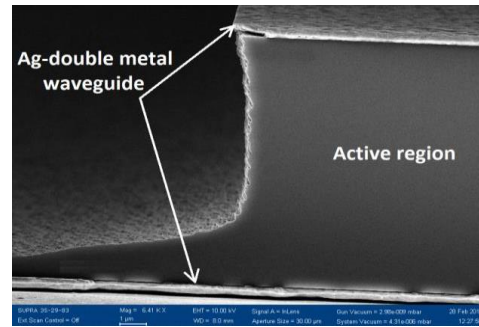


**Fig. 3.** SEM image of THz QCL with Ag-Ag double metal waveguide.

### Acknowledgements

This work was supported by the Russian Science Foundation (Project #18-19-00493).

### References

1. Han, Y. J., Li, L.H., Zhu, J., Valavanis, A., Freeman, J.R., Chen, L., Rosamond, M., Dean, P., Davies, A.G., Linfield, E.H. Silver-based surface plasmon waveguide for terahertz quantum cascade lasers // *Opt. Express*. 2018. V. 26, No.4. P. 3814–3827.
2. Khabibullin, R. A., Shchavruk, N. V., Pavlov, A. Y., Ponomarev, D. S., Tomosh, K. N., R. R. Galiev, Maltsev, P. P., Zhukov, A. E., Cirlin, G. E., Zubov, F. I., Alferov, Z. I. Fabrication of a terahertz quantum-cascade laser with a double metal waveguide based on multilayer GaAs/AlGaAs heterostructures // *Semiconductors*. 2016. V. 50, No. 10. P. 1377–1382.
3. Schrottko, L., Lu, X., Roben, B., Biermann, K., Wienold, M., Richter, H., Hubers, H.W., Grahn, H.T. Intrinsic frequency tuning of terahertz quantum-cascade lasers // *J. Appl. Phys*. 2018. V. 123, No. 21. P. 213102.
4. Khabibullin, R. A., Shchavruk, N. V., Ponomarev, D. S., Ushakov, D. V., Afonenko, A. A., Vasil'evskii, I. S., Zaycev, A. A., Danilov, A. I., Volkov, O. Yu., Pavlovskiy, V. V., Maremyanin, K. V., Gavrilenko, V. I. Temperature dependences of the threshold current and output power of a quantum-cascade laser emitting at 3.3 THz // *Semiconductors*. 2018. V. 52, No. 11. P. 1381–1386.
5. Khabibullin, R. A., Shchavruk, N. V., Klochkov, A. N., Glinskiy, I. A., Zenchenko, N. V., Ponomarev, D. S., Maltsev, P. P., Zaycev, A. A., Zubov, F. I., Zhukov, A. E., Cirlin, G. E., Alferov, Zh. I. Energy spectrum and thermal properties of a terahertz quantum-cascade laser based on the resonant-phonon depopulation scheme // *Semiconductors*. 2017. V. 51, No. 4. P. 514–519.
6. Reznik, R. R., Kryzhanovskaya, N. V., Zubov, F. I., Zhukov, A. E., Khabibullin, R. A., Morozov, S. V., Cirlin G. E. MBE growth, structural and optical properties of multilayer heterostructures for quantum-cascade laser // *Journal of Physics: Conf. Series*. 2017, V. 917. P. 052012
7. Ikonnikov, A. V., Maremyanin, K. V., Morozov, S. V., Gavrilenko, V. I., Pavlov, A. Yu., Shchavruk, N. V., Khabibullin, R. A., Reznik, R. R., Cirlin, G. E., Zubov, F. I., Zhukov, A. E., Alferov, Zh. I. Terahertz radiation generation in multilayer quantum-cascade heterostructures // *Technical Physics Letters*. 2017, V. 43, No. 4. P. 358–361.
8. Volkov, O. Yu., Dyuzhikov, I. N., Logunov, M. V., Nikitov, S. A., Pavlovskii, V. V., Shchavruk, N. V., Pavlov, A. Yu., Khabibullin, R. A. Analysis of terahertz radiation spectra in multilayer GaAs/AlGaAs heterostructures // *Journal of Communications Technology and Electronics*. 2018. Vol. 63, No. 9. P. 1042–1046.